Thermal characterization of a solid-solid phase change material for energy storage application

Adrien Abbate, Gregory Largiller, Fabrice Bentivoglio

Thermal characterization of a solid-solid phase change material for energy storage application

Adrien Abbate, Gregory Largiller and Fabrice Bentivoglio
Univ. Grenoble Alpes
CEA, LITEN, DTBH, LST
Grenoble, France
Gregory.largiller@cea.fr

***Abstract*—Thermal energy represents half of the primary energy used in Europe and is one of the main contributor of greenhouse gas emission. Integration of renewable thermal energy sources, such as biomass, solar thermal, geothermal or wasted heat is then a major stake for near future. Thermal Energy Storage (TES) is one of the key component that can help the development of renewable thermal energy in domains like urban heating network or industrial processes, allowing to smooth peaks of demand, to manage the balance with the supply and then to minimize the use of fossil energy.**

Most of the TES currently operated in the world are based on sensible heat by increasing and decreasing the temperature of a material such as water, thermal oil, molten salt, rock…

The use of Phase Change Materials (PCM) as storage medium enable to reach higher energy density for a large temperature range (i.e. 30°C to 1 000 °C [1]). Current technologies use solid-liquid phase PCM as TES medium and reach energy densities from 100 MJ.m^{-3} for paraffin to 1 000 MJ.m^{-3} for salt hydrates. These systems show some drawbacks like the presence of a liquid phase which may imply leakage, undercooling or large volume variation of about 10 to 20%V/V upon phase transformation [2] which leads to mechanical stresses for the storage vessel. An alternative solution consists in using solid-solid PCM with about 5-10%V/V phase change variation [1] and that could even later be used as structural material of the TES systems.

This study proposes to investigate and compare the thermal behavior of a classical solid-liquid paraffin and a polyalcohol as a solid-solid PCM. Both materials have first been analyzed by calorimetry and then characterized into a thermal bench.

The bench used is composed of two thermal loops, a heat exchanger with circular metallic fins composes the former test section. PCM fills the space between the fins. Temperature into the section is measured and used to calculate the heat flux and the energy stored into the system to compare the properties of the solid-solid PCM with the solid-liquid classical paraffin as reference. Latent heat, energy density and thermal conductivity are compared. Furthermore, several thermal cycles are done to study the effect of the aging on both materials.

Keywords—Phase Change Materials (PCM); Thermal Energy Storage (TES); Solid-Solid PCM

I. INTRODUCTION

Thermal energy storage (TES) is a key component for a better integration of renewable energy, such as biomass, solar thermal, geothermal or wasted heat, in heating processes. Indeed, either dealing with daily, seasonal temperature or natural demand variations, thermal energy storage allows to smooth peaks of demand and manage the balance with supply to minimize energy losses, decrease the use of fossil combustible commonly used to manage peak demands. The potential of TES is high thanks to a large range of applications such as urban districts networks, buildings and industrial processes using heat [3].

Thermal energy is commonly stored using sensible heat with like water, thermal oils, molten salts, rocks…. TES using latent heat presents two main advantages: the storage works at constant temperature depending on the PCM (i.e. 30°C to 1 000 °C) and a large energy density can be reached thanks to a latent heat from 200 MJ.m^{-3} for paraffin to 600 MJ.m^{-3} for salt hydrates [1]. Therefore, compact TES can be designed with a working temperature dedicated to the application.

Several criteria influence the choice of the PCM such as the latent heat and the temperature of transition but also the thermal conductivity and the volume variation due to the phase change [4]. Common technologies use solid-liquid PCMs owing to large energy density and wide variety of materials. However, liquid phase implies some drawbacks known as potential leakage and large volume variation (around 10-20%V/V [3]) leading to mechanical stresses on structures. An improvement would consist of using solid-solid PCM which have less than 10%V/V phase change variation [5]. Thanks to their solid state, there is no possible leakage and no encapsulation is required. Solid-solid PCM can therefore be used as structural materials[6]–[8] for the TES systems or be charged to make composite materials like concrete [9].

In this study, thermal behavior of two PCMs are investigated: the RT70-HC, a classical commercial solid-liquid and the Tris(hydroxymethil)aminomethane (TRIS) a polyalcohol with solid-solid transition. These materials are characterized by calorimetry (around 5 g samples) then into a thermal test bench (about 1.5 kg samples).

978-1-7281-3923-4/19/$31.00 ©2019 European Union

In this paper, the experimental test bench is presented in section 2. The temperatures in the PCMs are recorded during several thermal cycles for both materials; characteristics and results are discussed in section 3.

II. Experimental Setup and Method

A. Overview of the test bench

The test bench is composed of two thermal loops (Process Instrumentation Diagram, Fig. 1) the heat transfer fluid (HTF) - i.e. thermal oil with a specific heat around 1.8 kJ.K^{-1}.kg^{1} - circulates through two thermal baths. *Julabo* thermal baths are W40 series with a heating power of 2.7 kW and a pressure up to 1.7 bar at the pump outlet. The facility works for a temperature up to 255 °C and for a flow up to 60 kg.h^{-1}. Therefore, the available power can reach 7 kW which is enough for the charge of the two PCMs selected in this study. Two four-way valves conduct the HTF into the exchanger or through the bypass.

The test section is made of a cylindrical heat exchanger filled out with PCMs. The fins are of 57 mm in diameter helically mounted on a 25.4 mm tube (thickness of 0.37 mm, fins interval of 2 mm). Aluminum fins strongly improve the conductive radial heat flux thanks to a high thermal conductivity (220 W.m^{-1}.K^{-1} against around 0.2 W.m^{-1}.K^{-1} for the PCMs). The total free volume was calculated and verified with water filling to 1.6 L.

The step when the PCM stores heat is named the charge and the step when the PCM releases heat is named the discharge. The coolant flows from the up to the down during the charge process and from the bottom to the top during the discharge process. Several thermal charge/discharge cycles are done during few days to investigate the PCM and the system behavior.

B. Materials characteristics and method

Materials are characterized with a Tian-Calvet C80 calorimeter supplied by *Setaram*, that is specified to 7% accuracy. To measure the phase transition enthalpy, a stainless steel cell is filled with a measured mass m of material. The cell is placed in the calorimeter next to a same empty cell as reference. The calorimeter heats cells at $\frac{dT}{dt}$ = 0.02 K.min^{-1} and measures the heat flux mismatch $\Delta\Phi$ between the two cells. To substract the equipment contribution, a blank test is previously made with two empty cells. Equation (1) and (2) show, respectively, how the specific equivalent heat, c_p, and the enthalpy, h, are calculated.

$$c_p(T) = \frac{\Delta\Phi}{m\frac{dT}{dt}} \quad (1)$$

$$h(T) - h_{ref} = \int_{Tref}^{T} c_p(T)dT \quad (2)$$

Where h_{ref} is the reference enthalpy (equal to zero) for the reference temperature, T_{ref}.

The first PCM characterized is the RT70-HC, a commercial PCM provided by *Rubitherm Gmbh* and specially made for TES application. According to *Rubitherm*, this material has a melting temperature between 69°C and 71 °C and a latent heat of fusion of 260 kJ.kg^{-1}. The density is 880 kg.m^{-3} for the solid phase and 770 kg.m^{-3} for the liquid phase. Therefore, RT70-HC enables an energy density around 196 MJ.m^{-3} for the liquid. These thermal characteristics are verified thanks to the enthalpy curve obtained by calorimetry on Fig. 2. This curve shows a melting temperature from 69 °C to 74 °C and a latent heat of 255 kJ.kg^{-1}.

The second PCM characterized is the Tris(hydroxymethil)aminomethane ($C_4H_{11}NO_3$), commonly known as TRIS, Trometanol, THAM or TAM, which is a spherical molecule generally used as a buffering agent in the pH range of 7-9 and is for example used in seawater studies [10]. This material has been identified as a potential efficient PCM because of its solid-solid phase change with a large latent heat (from 270 J.g^{-1} [11] to 285 J.g^{-1} [12] according to different authors) at temperatures around 135°C and a good chemical stability [12], [13]. Thanks to these characteristics, TRIS is a suitable candidate for industrial applications such as organic Rankine cycle (ORC) system and waste heat recovery system [14]. Trometanol is a common commercial material usually used in small quantities. According to the datasheet, the absolute solid density is 1353 kg.m^{-3} in normal conditions. The measured bulk density is 881 kg.m^{-3} which corresponds to a compactness of 65%vol/vol. Therefore, the energy density is 238 MJ.m^{-3} in powder form and reaches 365 MJ.m^{-3} for a fully dense material.

Like many spherical molecules, TRIS exhibits a solid-solid transition before melting [10]. It changes from a low temperature ordered crystalline structure to a high temperature crystalline phase, known as “plastic crystal”. TRIS moves from orthorhombic crystal to a BCC structure in a range temperature from 133 °C to 140 °C [12].

These thermal characteristics are verified on the enthalpy curve obtained by calorimetry on Fig. 3. This curve shows a melting temperature from 134 °C to 139 °C and a latent heat of 278 kJ.kg^{-1}. Characteristics of the two PCMs are summarized in TABLE I.

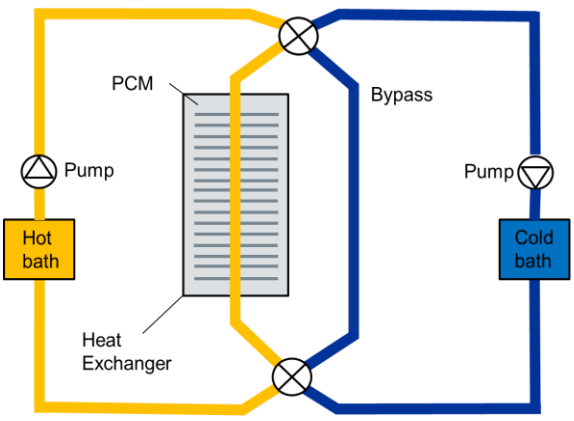

Fig. 1. Schematic of the test bench

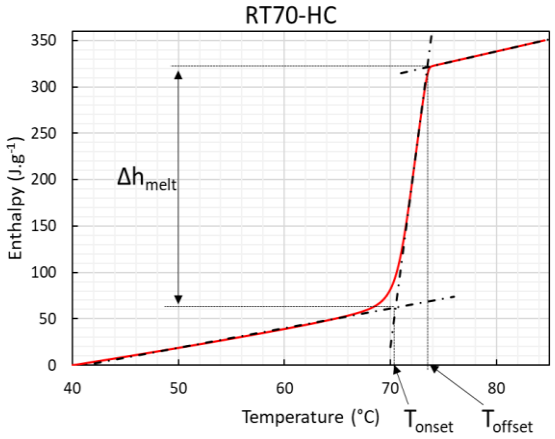

Fig. 2. Specific heat of the RT70-HC (calorimetry)

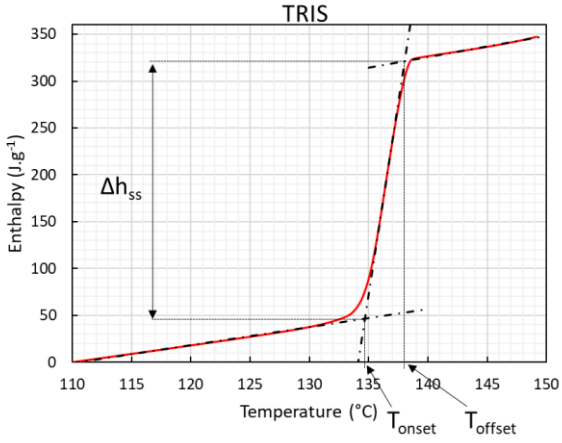

Fig. 3. Specific heat of the TRIS (calorimetry)

TABLE I. CHARACTERISTICS FOR THE TWO MATERIALS

Material	**T_{onset}** (°C)	**T_{offset}** (°C)	**Latent heat** (kJ.kg^{-1})	**Density** (kg.m^{-3})		**Energy density** (MJ.m^{-3})
RT70-HC	69	74	255	Bulk powder	880	224
				Liquid	770	196
TRIS	134	139	278	Fully dense	1353	365
				Bulk powder	881	238

To estimate the heat transfer with the HTF in the test section, each loop has a flowmeter and two thermocouples placed upstream and downstream the test section. Energy balance gives the heat released or absorbed in the heat exchanger, eq (3) where Φ_{FC} the heat flux, c_p the HTF specific heat, T_{in} and T_{out} the inlet and outlet temperature and $\dot{q}$ the flow. The total heat transferred has further to consider losses into metallic parts of the section and exchanges to the environment.

$$\Phi_{FC} = \dot{q} c_p (T_{out} - T_{in}) \quad (3)$$

To evaluate the energy stored in the PCM, 40 thermocouples are placed inside the tank. The heat exchanger is discomposed into five axial sections (from A to E), two radial rings (in and out) and four quarter (from 0° to 270°), cf. Fig. 4. A thermocouple is placed in every mesh. Since the system is axisymmetric, the average temperature is considered for each ring. Therefore, knowing the PCM density, the metallic mass repartition of the tubes and fins, the theoretical heat stored into the tank can be calculated thanks to the enthalpy measured by calorimetry.

III. Results and Discussion

A. RT70-HC

The test section is filled with 1.3 kg of PCM at liquid state. This mass corresponds to a latent heat storage capacity of 331 kJ in the PCM. Five thermal cycles of charge and discharge are performed. To operate a charge, the PCM is stabilized at a temperature around 40 °C, then the HTF preheated at 90°C flows through the inner tube of the test section from up to down at a flow of 12 kg.h^{-1} for the first cycle and 20 kg.h^{-1} for the last one. To perform a discharge, the PCM is stabilized at 90°C then the HTF cooled down at 40°C or 50°C flows through the inner tube from down to up at a flow around 13 kg.h^{-1} for every test.

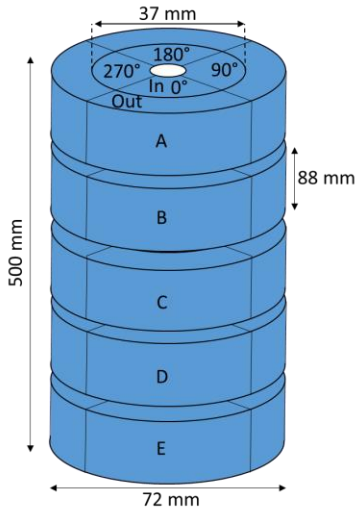

Fig. 4. Experimental meshing of the test section showing the thermocouple positions

Temperature evolutions of the first charge are plotted on Fig. 5 and on Fig. 6 for the last charge. These two experimental sets are very similar despite the difference of inlet HTF flow. RT70-HC seems to have a good stability after five thermal cycles. All temperature profiles show a temperature plateau around 70°C which corresponds to the phase change. In the test section, the PCM melts from up to down and the radius has not a strong impact on the melting rate because of the radial fins. Conversely, the phase change rate strongly depends on the axial position. Indeed, the PCM rapidly melts near the HTF inlet because of the large heat input which absorbs energy: Near the outlet, the melting rate is slower but is also impacted by the thermal phenomenon upstream. While the section A melts, it absorbs a large amount of heat from the HTF, impacting sections downstream which heat up slower because of lower HTF temperature (visible on section E temperature profile around 60 °C). This phenomenon happens during the section A temperature plateau à 70°C. The HTF temperature strongly falls downstream which implies the heat flux decrease between the HTF and the PCM in section E (Fig. 7).

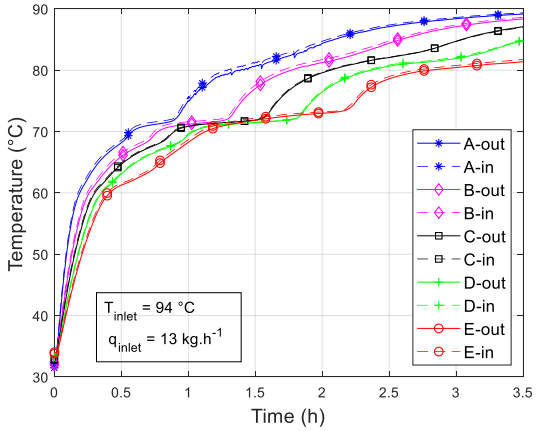

Fig. 5. Temperature evolution in the RT70-HC for the first charge

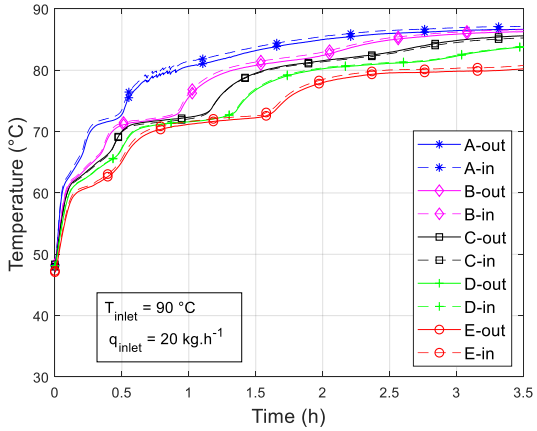

Fig. 6. Temperature evolution in the RT70-HC for the last charge

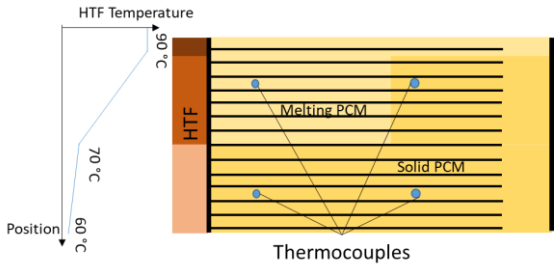

Fig. 7. Influence of the upstream PCM melt on the downstream heat flux

Fig. 8 and Fig. 9 show temperature profiles for the first and the last discharge, respectively. A temperature plateau is visible at 70°C like for the charges - the transformation is reversible as expected. However, a second temperature plateau appears around 60°C. This plateau is due to the slow solidification between the fins and the outside cylinder. As illustrated in the Fig. 10, since the heat flux is mainly transported by conduction through aluminum fins and solid PCM, the temperature, T, is given by the heat equation (4), where λ is the thermal conductivity, ρ the density, c_p the specific heat, r the radial position and t the time. In addition, the heat flux, Φ, between the molten PCM and the HTF through the solid PCM depends on the thermal resistance, R_{th}, and the temperature difference, ΔT, with the HTF, equation (5). This thermal resistance increases with the progress of the fusion front, $r(t)$, equation (6) inside fins and equation (7) outside fins, where r_0 is the external tube radius and L a characteristic length. The equivalent thermal conductivity of

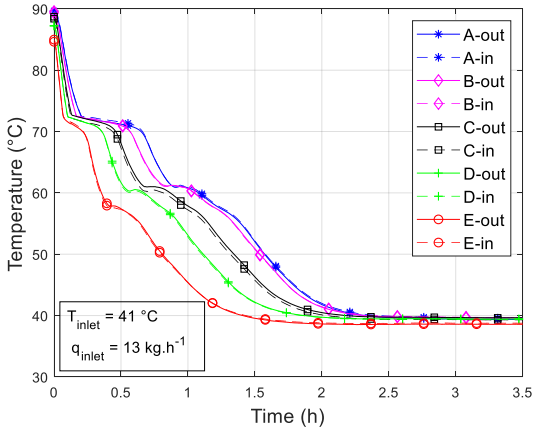

Fig. 8. Temperature evolution in the RT70-HC for the first discharge

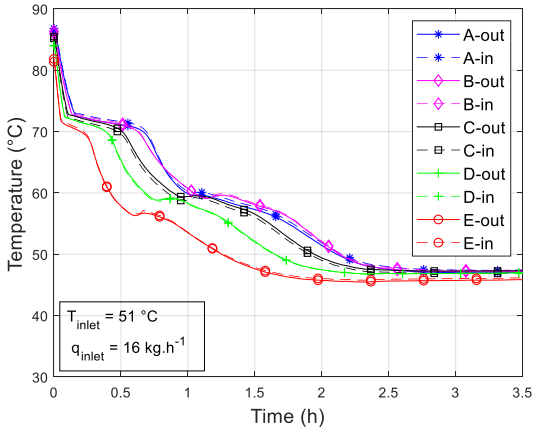

Fig. 9. Temperature evolution in the RT70-HC for the last discharge

the PCM and fins has been estimated using 2D axisymmetric conduction calculation, the value is about 10 $W.m^{-1}.K^{-1}$ [15]. The heat conductivity of pure RT-70HC is around 0.2 $W.m^{-1}.K^{-1}$ according to its data sheet. This drop of the thermal conductivity at the end of the fins leads to a sudden rise of the thermal resistance, as visible on the Fig. 11. Therefore, since thermocouples are between two fins, when the solidification is complete in the inter fins area, the temperature rapidly decreases. However, when the outside PCM starts to melt, the temperature in this area is fixed and the heat flux between the HTF and the fusion front is low because of the new high thermal resistance, eq. (7). This implies a stabilization of the recorded temperature; a second plateau appears, as illustrated on the Fig. 12. The temperature decreases again when the whole PCM is solid and reaches the HTF temperature.

$$\frac{\partial T}{\partial t} = \frac{\lambda}{\rho.Cp}.\frac{1}{r}.\frac{\partial}{\partial r}r\frac{\partial T}{\partial r} \tag{4}$$

$$\Delta T = R_{th}\,\Phi \tag{5}$$

$$R_{th} = \frac{\ln\left(\frac{r(t)}{r_0}\right)}{2\pi L\,\lambda_{PCM+fins}} \tag{6}$$

$$R_{th} = \frac{\ln\left(\frac{r_{fin}}{r_0}\right)}{2\pi L\, \lambda_{PCM+fins}} + \frac{\ln\left(\frac{r(t)}{r_{fin}}\right)}{2\pi L\, \lambda_{PCM}} \quad (7)$$

B. TRIS

In the case of solid-solid PCM, one cannot fill the test section in liquid phase without irreversibly degrade the PCM. In order to insert powder between each fins, the tank is filled by the side with 1.4 kg of TRIS, see Fig. 13. This mass corresponds to a latent heat storage capacity of 389 kJ in the PCM, 17% more than the RT70-HC. The porosity of the PCM reaches 65%vol/vol inside the test section which is the commonly accepted packing density for a granular material. To charge the PCM, HTF at 150°C flows through the inner tube of the test section from up to down with a flow of 9 kg.h^{-1}. To discharge the PCM, HTF at 95°C flows through the inner tube from down to up at a flow around 10 kg.h^{-1}.

For the first cycles with TRIS, the temperature plateau, typical of a phase transition, is not clearly visible. It is visible only for section A to D. This is due to the HTF inlet temperature which was only at 134°C, too close to the transition temperature. The wanted HTF inlet temperature is 150 °C, but unfortunately, this temperature was not reached for the first and the second tests because of the thermal losses along the loop, which are high at this level of temperature. So, only the last cycle is considered for the discussion.

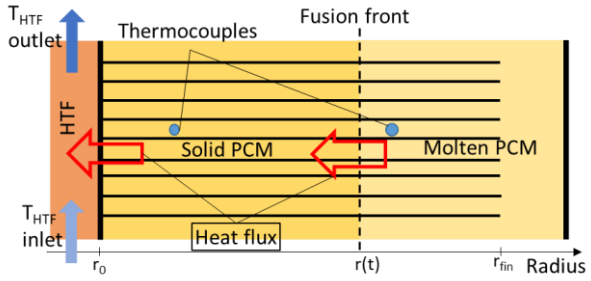

Fig. 10. Schematic of the thermal phenomenon during the temperature rate reduction around 60°C

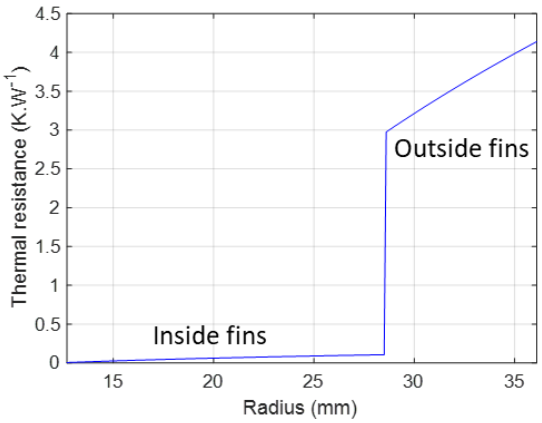

Fig. 11. Thermal resistance with and without aluminum fins

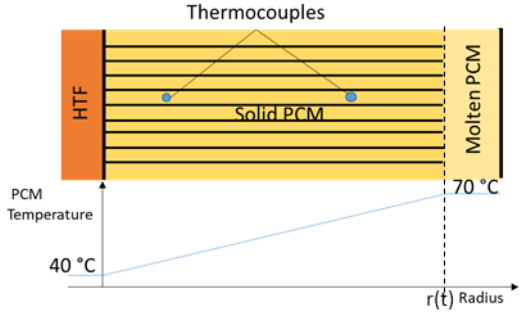

Fig. 12. Schematic of the thermal phenomenon during the temperature rate reduction around 60°C

The inlet temperature for the last charge was 155 °C. Temperature plateau are visible around 134 °C, consequence of the phase transition (see Fig. 14). This charge can be compared to the first charge of the RT70-HC, flow rates (around 10 kg.h^{-1}) and temperature differences between HTF inlet temperature and melting temperature (around 20 °C) are similar. For the TRIS, time required to reach the phase change is less than 1h for section A and less than 2.5h for section E. In addition, the time to finish melting the whole PCM are close to the RT70-HC. Taking into account that the experimental conditions are very similar for both cases and that the volumetric specific heat, ρc_p, are similar for RT70-HC and TRIS (respectively 1 760 kJ.K^{-1}.m^{-3} and 1 560 kJ.K^{-1}.m^{-3}), the latent heats and equivalent thermal conductivities are close for RT70-HC and TRIS (equation 4). In a heat exchanger with metallic fins, the thermal conductivity is mainly imposed by the fins as explained in section II.

Fig. 15 shows temperature profiles for the last discharge. The temperature of the PCM decreases below the transition temperature, down to 118 °C, 16°C under the transition temperature, and then increase up to a temperature plateau between 124°C and 129 °C, for the section E and for the section B, respectively. This phenomenon is due to the PCM undercooling and has been observed in at least one previous study [16]. In their paper, Zhai *et al.* [16] note an undercooling of 63 °C for TRIS. In addition, another experiment was made, a TRIS sample is placed in an oven under nitrogen, heated up to 143 °C and then cooled down to 108 °C. In these conditions, an undercooling of 8 °C is observed. The temperature record of this experiment is visible on the Fig. 16. Undercooling depends on various effects such as homogenous, heterogeneous nucleation or cooling rate. So, the transition is reversible but not at always at the same temperature.

C. Aging of the solid-solid PCM

According to the chemical composition of a PCM, several mechanisms like segregation or oxidation can modify its thermal properties. On a given application, users have to estimate the lifespan of the material in real conditions by taking into account the physical or chemical mechanisms which may be implied [17]. Studies show that sugar alcohol like TRIS are more sensitive to oxidation than fatty acid because of the interaction of the hydroxyl group with oxygen [18]–[20]. For new potential PCMs, effects of aging on materials are sometimes investigated with DSC and FTIR before and after fast thermal cycling [21]–[23]. According to the application, some authors focus on the time of exposure at high temperature [18], [24], others on the number of thermal cycle before noticeable degradation [25] or interactions with containers [26], [27]. As far as authors know, the scientific community did not agree on a standardization method to qualify aging of PCMs [28].

Five thermal cycles from 90 °C to 150 °C were done from 90°C to 150°C on the TRIS during nearly 200h under air. The temperature profile is presented on Fig. 17. This corresponds

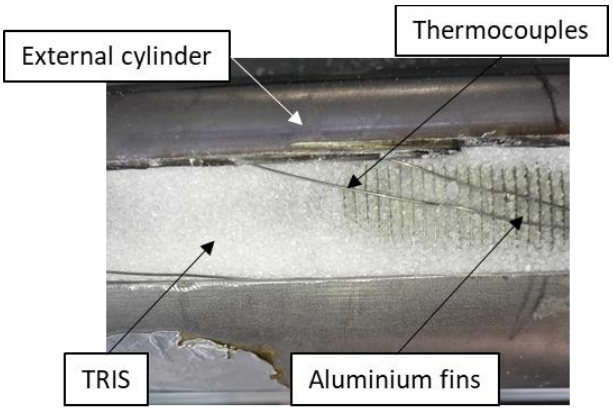

Fig. 13. Test section filled with TRIS

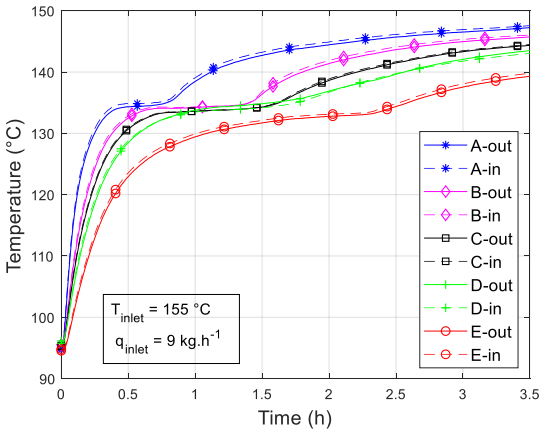

Fig. 14. Temperature evolution in the TRIS for the last charge

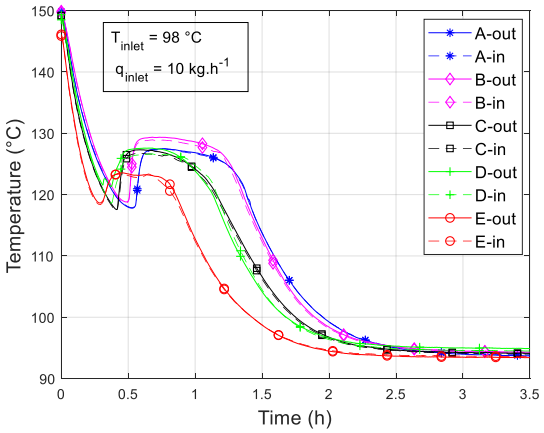

Fig.15. Temperature evolution in the TRIS for the last discharge

to a cumulated time above the transition temperature of 32h. After thermal treatment, one observes sintered grains, a global swelling (Fig. 18) where the material turned from white to brown which typical of temperature activated oxidation of sugars alcohol.

Calorimetry experiment was done on a TRIS sample from the test section after five cycles, in a stainless steel cell under air. The enthalpy curves of the old TRIS versus the new TRIS are plotted on Fig. 19. The transition latent heat has decreased from 278 kJ.kg^{-1} to 238 kJ.kg^{-1}, a loss of 14% in only five cycles. This loss of 14% relevant even considering the uncertainties of 7% of the C80 calorimeter. In addition, the transition temperature has dropped from 134°C to 133.5 °C.

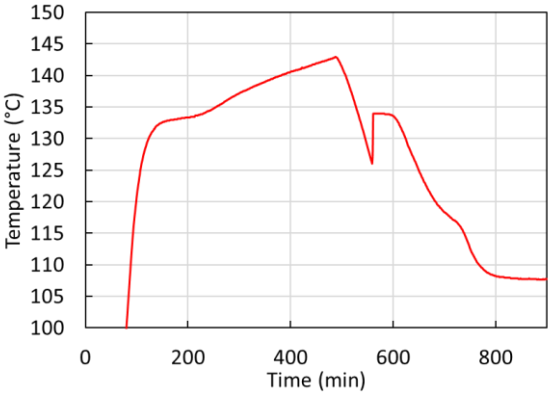

Fig. 16. Temperature evolution of TRIS in oven under nitrogen

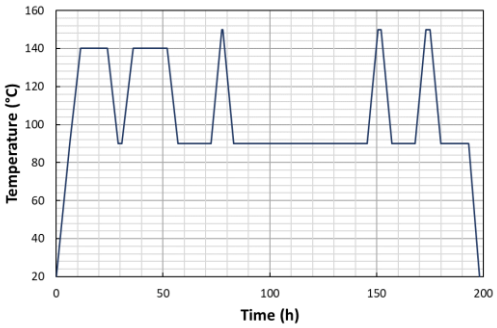

Fig. 17. Temperature profile of PCM temperature during 5 thermal cycles

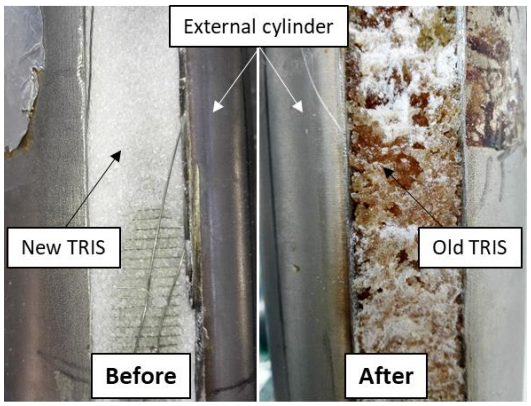

Fig. 18. TRIS before and after five thermal cycles

Another experiment has been done to investigate the TRIS aging. A sample of new TRIS is placed in a hermetically closed vessel and heated up in an oven at 150 °C during 200h under nitrogen. Enthalpy curves after thermal treatment are plotted on Fig. 20. TRIS does not present a distinct phase transition as observed previously; A transition latent heat of 150 kJ.kg^{-1} can hardly be measured. It corresponds to a loss of 46%. The final enthalpy at 150 °C decreases to 290 kJ.kg^{-1} instead of 350 kJ.kg^{-1}, which corresponds to a drop of 17%. The experiment was under nitrogen atmosphere, the oxidation might not be responsible for these changes. Other mechanisms can be the cause of this deterioration and have to be investigated.

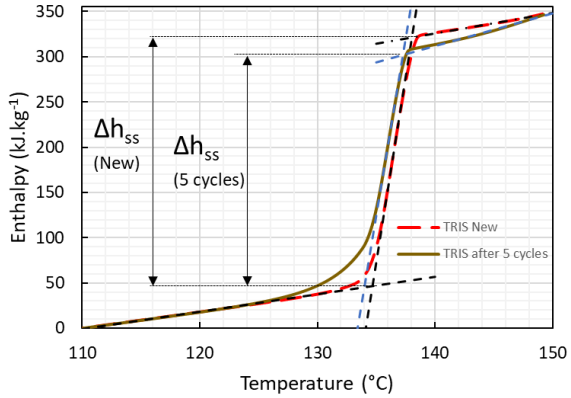

Fig. 19. Enthalpy variation of the TRIS after five thermal cycle

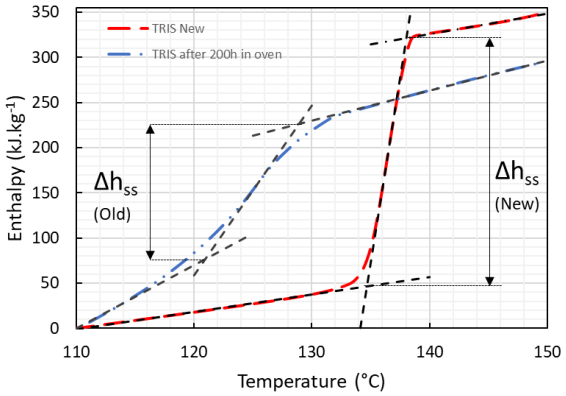

Fig. 20. Calorimetry of the TRIS after 200h in oven at 150°C under nitrogen

IV. Conclusion

TRIS has a great potential to become a solid-solid PCM thanks to a large latent heat and low temperature transition, which is appropriated for applications such as urban heating network or housing. In this paper, thermal behavior of TRIS in a 1.6 L tank during five thermal cycles is studied. The comparison of this solid-solid PCM with classical solid-liquid PCM shows good similarities for thermal behavior but also some issues for the TRIS. Indeed, TRIS being in powder state, porosity remains and the PCM does not occupy fully the available volume. Also, the TRIS is not perfectly stable under air and loses its thermal characteristics with time. Even if after ageing of 32h the latent heat of phase transition is not totally degraded and remains around 250 $kJ.kg^{-1}$, the temperature of phase transition decreases and spreads. Therefore, future tests are needed to investigate the evolution of the thermal energy storage capacity: denser materials should be tested and further work on ageing should be performed. A new test section is under construction to limit thermal losses and improve energy balance determination.

References

[1] A. Fallahi, G. Guldentops, M. Tao, S. Granados-Focil, et S. Van Dessel, « Review on solid-solid phase change materials for thermal energy storage: Molecular structure and thermal properties », *Appl. Therm. Eng.*, vol. 127, p. 1427-1441, déc. 2017.

[2] L. F. Cabeza, A. Castell, C. Barreneche, A. de Gracia, et A. I. Fernández, « Materials used as PCM in thermal energy storage in buildings: A review », *Renew. Sustain. Energy Rev.*, vol. 15, nº 3, p. 1675-1695, avr. 2011.

[3] P. Arce, M. Medrano, A. Gil, E. Oró, et L. F. Cabeza, « Overview of thermal energy storage (TES) potential energy savings and climate change mitigation in Spain and Europe », *Appl. Energy*, vol. 88, nº 8, p. 2764-2774, août 2011.

[4] M. M. Kenisarin et K. M. Kenisarina, « Form-stable phase change materials for thermal energy storage », *Renew. Sustain. Energy Rev.*, vol. 16, nº 4, p. 1999-2040, mai 2012.

[5] J. Font, J. Muntasell, et E. Cesari, « Plastic crystals: Dilatometric and thermobarometric complementary studies », *Mater. Res. Bull.*, vol. 30, nº 7, p. 839-844, juill. 1995.

[6] W. F. Gao, W. X. Lin, T. Liu, et M. Li, « An experimental study on the application of polyalcohol solid-solid phase change materials in solar drying with cross-corrugated solar air collectors », présenté à IOP Conference Series: Earth and Environmental Science, 2017, vol. 93.

[7] M. Barrio, J. Font, D. O. López, J. Muntasell, et J. L. Tamarit, « Floor radiant system with heat storage by a solid-solid phase transition material », *Sol. Energy Mater. Sol. Cells*, vol. 27, nº 2, p. 127-133, juill. 1992.

[8] M. Kuta et T. M. Wójcik, « Phase change materials in energy sector - applications and material requirements », *EPJ Web Conf.*, vol. 92, p. 02043, 2015.

[9] X. Li *et al.*, « Experimental investigation of thermal and mechanical properties of magnesium oxychloride cement with form-stable phase change material », *Constr. Build. Mater.*, vol. 186, p. 670-677, oct. 2018.

[10] D. Eilerman et R. Rudman, « Polymorphism of crystalline poly(hydroxymethyl) compounds. III. The structures of crystalline and plastic tris(hydroxymethyl)aminomethane », *J. Chem. Phys.*, vol. 72, nº 10, p. 5656-5666, mai 1980.

[11] M. Barrio *et al.*, « Miscibility and molecular interactions in plastic phases: Binary system pentaglycerin/ tris(hydroxymethyl)aminomethane », *J. Phys. Chem. Solids*, vol. 54, nº 2, p. 171-181, févr. 1993.

[12] R. Shi, D. Chandra, A. Mishra, A. Talekar, M. Tirumala, et D. J. Nelson, « Thermodynamic reassessment of the novel solid-state thermal energy storage materials: Ternary polyalcohol and amine system pentaglycerine-tris(hydroxymethyl)-amino-methane-neopentylglycol (PG-TRIS-NPG) », *Calphad*, vol. 59, p. 61-75, déc. 2017.

[13] J. Timmermans, « Plastic crystals: A historical review », *J. Phys. Chem. Solids*, vol. 18, nº 1, p. 1-8, janv. 1961.

[14] C.-B. Wu *et al.*, « Preparation of microencapsulated medium temperature phase change material of Tris(hydroxymethyl)methyl aminomethane@SiO2 with excellent cycling performance », *Appl. Energy*, vol. 154, p. 361-368, sept. 2015.

[15] M. Martinelli, « Stockage d'énergie thermique par changement de phase – Application aux réseaux de chaleur », Grenoble Alpes, 2016.

[16] M. Zhai, S. Zhang, J. Sui, F. Tian, et X. Z. Lan, « Solid–solid phase transition of tris(hydroxymethyl)aminomethane in nanopores of silica gel and porous glass for thermal energy storage », *J.*

Therm. Anal. Calorim., vol. 129, nº 2, p. 957-964, août 2017.

[17] A. Abhat, « Low temperature latent heat thermal energy storage: Heat storage materials », *Sol. Energy*, vol. 30, nº 4, p. 313-332, janv. 1983.

[18] H. Neumann *et al.*, « Thermal stability enhancement of d-mannitol for latent heat storage applications », *Sol. Energy Mater. Sol. Cells*, vol. 200, p. 109913, sept. 2019.

[19] A. Solé, H. Neumann, S. Niedermaier, I. Martorell, P. Schossig, et L. F. Cabeza, « Stability of sugar alcohols as PCM for thermal energy storage », *Sol. Energy Mater. Sol. Cells*, vol. 126, p. 125-134, juill. 2014.

[20] G. Raam Dheep et A. Sreekumar, « Thermal reliability and corrosion characteristics of an organic phase change materials for solar space heating applications », *J. Energy Storage*, vol. 23, p. 98-105, juin 2019.

[21] N. Zhang, Y. Song, Y. Du, Y. Yuan, G. Xiao, et Y. Gui, « A Novel Solid–Solid Phase Change Material: Pentaglycerine/Expanded Graphite Composite PCMs », *Adv. Eng. Mater.*, vol. 20, nº 10, p. 1800237, 2018.

[22] K. P. Venkitaraj, S. Suresh, et A. Venugopal, « Experimental study on the thermal performance of nano enhanced pentaerythritol in IC engine exhaust heat recovery application », *Appl. Therm. Eng.*, vol. 137, p. 461-474, 2018.

[23] C. R. Raj, S. Suresh, R. R. Bhavsar, V. K. Singh, A. S. Reddy, et A. Upadhyay, « Manganese-based layered perovskite solid–solid phase change material: Synthesis, characterization and thermal stability study », *Mech. Mater.*, vol. 135, p. 88-97, août 2019.

[24] R. I. Olivares et W. Edwards, « LiNO3–NaNO3–KNO3 salt for thermal energy storage: Thermal stability evaluation in different atmospheres », *Thermochim. Acta*, vol. 560, p. 34-42, mai 2013.

[25] S. D. Sharma, D. Buddhi, et R. L. Sawhney, « Accelerated thermal cycle test of latent heat-storage materials », *Sol. Energy*, vol. 66, nº 6, p. 483-490, sept. 1999.

[26] L. Calabrese, V. Brancato, V. Paolomba, et E. Proverbio, « An experimental study on the corrosion sensitivity of metal alloys for usage in PCM thermal energy storages », *Renew. Energy*, vol. 138, p. 1018-1027, août 2019.

[27] G. Mohan, M. B. Venkataraman, et J. Coventry, « Sensible energy storage options for concentrating solar power plants operating above 600 °C », *Renew. Sustain. Energy Rev.*, vol. 107, p. 319-337, juin 2019.

[28] G. Ferrer, A. Solé, C. Barreneche, I. Martorell, et L. F. Cabeza, « Review on the methodology used in thermal stability characterization of phase change materials », *Renew. Sustain. Energy Rev.*, vol. 50, p. 665-685, oct. 2015.